THE JOURNAL OF PHYSICAL CHEMISTRY A

Article

pubs.acs.org/JPCA

Experiment and Theory Elucidate the Multichannel Predissociation Dynamics of the HCl Trimer: Breaking Up Is Hard To Do

John S. Mancini,[†] Amit K. Samanta,[‡] Joel M. Bowman,*[,†] and Hanna Reisler*[,‡]

[†]Department of Chemistry and Cherry L. Emerson Center for Scientific Computation, Emory University, Atlanta, Georgia 30322, United States

[‡]Department of Chemistry, University of Southern California, Los Angeles, California 90089, United States

Ⓦ *Web-Enhanced Feature* Ⓢ *Supporting Information*

ABSTRACT: The breaking of hydrogen bonds in molecular systems has profound effects on liquids, e.g., water, biomolecules (e.g., DNA), etc., and so it is no exaggeration to assert the importance of these bonds to living systems. However, despite years of extensive research on hydrogen bonds, many of the details of how these bonds break and the corresponding energy redistribution processes remain poorly understood. Here we report extensive experimental and theoretical insights into the breakup of two or three hydrogen bonds of the dissociation of a paradigm system of a hydrogen-bonded network, the ring HCl trimer. Experimental state-to-state vibrational predissociation dynamics of the trimer following vibrational excitation were studied by using velocity map imaging and resonance-enhanced multiphoton ionization, providing dissociation energies and product state distributions for the trimer's breakup into three separate monomers or into dimer + monomer. Accompanying the experiments are high-level calculations using diffusion Monte Carlo and quasiclassical simulations, whose results validate the experimental ones and further elucidate energy distributions in the products. The calculations make use of a new, highly accurate potential energy surface. Simulations indicate that the dissociation mechanism requires the excitation to first relax into low-frequency motions of the trimer, resulting in the breaking of a single hydrogen bond. This allows the system to explore a critical van der Waals minimum region from which dissociation occurs readily to monomer + dimer.

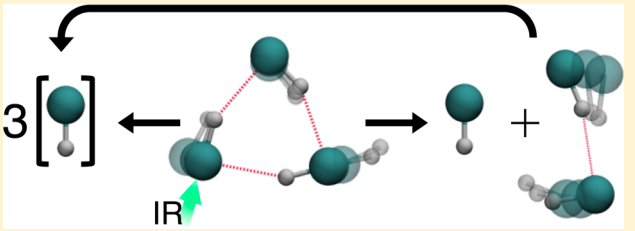

I. INTRODUCTION

The hydrogen bond (H-bond) is the most pervasive bond in nature. It holds the strands of DNA together[1] as well as provide the "glue" for water.[2] Not surprisingly all aspects of this bond, including its formation and breakup, have been of ongoing interest to both theoreticians and experimentalists for over a century.[3−6] This desire to understand H-bonding has prompted the study of several paradigm systems for which the energetics and dynamics can be interrogated exhaustively, with the bulk of the work focused on dimers of water and other small hydride molecules.[7−18] Recently, impressive progress has been made toward detailed studies of prototypical H-bonded systems larger than dimers.[19−28] These studies stand to reveal much more about the dissociation dynamics of H-bonded networks and the cooperative nature of these interactions.

The hydrogen chloride trimer, $(HCl)_3$, is an ideal prototype for such detailed studies.[25−35] Each of the three HCl monomers of the trimer can accept and donate one hydrogen bond forming an effective "closed shell" of H-bonds in a stable triangularly bound geometry.[30] This configuration, due to its symmetry, is characterized by a single infrared active H−Cl stretch frequency. The stretch fundamental frequency has been measured with high-resolution spectroscopy in the gas phase at 2810 cm^{-1} [27,28] and recently determined with ab initio anharmonic analysis.[36,37] With this excitation energy, dissociation can occur via two channels with excitation of just the H−Cl stretch fundamental.[36] Breaking two hydrogen bonds leads to dimer + monomer fragments (Channel I), whereas breaking of three hydrogen bonds generates directly three monomers (Channel II). As will be shown below, the dissociation energies for these two channels are ∼1100 and ∼1500 cm^{-1}, respectively. Sequential dissociation in which internally "hot" dimers formed in Channel I break up can also produce HCl monomers.

In this study we combine quasiclassical trajectory (QCT) calculations with experiment, namely high-resolution and state-specific velocity map imaging (VMI), to describe, for the first time, the evolution of an H-bonded trimer from initial vibrational excitation to fragment internal and translational energy distributions. The complementary strengths of theory and experiment are enlisted to describe both energy transfer pathways and dissociation dynamics to multiple channels. We are able to determine accurate dissociation energies for channels I and II as well as the contributions of sequential

Special Issue: A. W. Castleman, Jr. Festschrift

Received: February 13, 2014
Revised: February 20, 2014

   dx.doi.org/10.1021/jp5015753 | J. Phys. Chem. A XXXX, XXX, XXX−XXX

dissociation processes and three-body cooperative interactions. Accurate determinations of these dissociation energies are accomplished using quantum diffusion Monte Carlo (DMC) calculations. The calculations rely on the existence of an accurate potential energy surface (PES) for the trimer, which has been recently reported by Mancini and Bowman and tested by calculating anharmonic vibrational energies of $(HCl)_3$ and short-time, nondissociative vibration-to-vibration (V−V) energy transfer.[36] The VMI technique has been exploited before to determine accurate values of bond dissociation energies (D_0) of dimers, which were in excellent agreement with theory, as well as correlated product state distributions.[8−11,17,18] This is the first time that VMI is applied with the same accuracy to the multichannel dissociation of a trimer and the results compared directly to high-level calculations.

II. EXPERIMENTAL DETAILS

The HCl trimer was generated in a pulsed supersonic molecular beam by expanding a mixture of 3.5% HCl and 10% Argon in Helium (backing pressure of 2 atm) through the 0.5 mm orifice of a pulsed valve (∼150 μs opening time) operating at 10 Hz. HCl concentration and backing pressure were optimized to maximize signal from the trimer and minimize formation of higher clusters. Caution was exercised to avoid water contamination during sample preparation or in the gas lines as the more strongly bound complexes of HCl with water create a broad background in the IR spectrum.

Vibrational predissociation (VP) of $(HCl)_3$ was studied following pulsed IR excitation. Rotationally excited HCl fragments were ionized by (2+1) resonance-enhanced multiphoton ionization (REMPI) and detected using time-of-flight (TOF) mass spectrometry and VMI. Details of the experimental procedures can be found in our previous publications.[8−11,17,18,20]

In brief, a skimmed molecular beam of the trimer was intersected at right angles by two counterpropagating IR and UV laser beams. The IR radiation in the H−Cl stretch region of the trimer (2810 cm^{-1})[27,28] was generated using an OPO/OPA system. IR frequencies were calibrated by measuring the well-known absorption spectrum of the HCl monomer. IR power (1 mJ/pulse, ∼0.4 cm^{-1} width) and focusing conditions (40 cm focal length lens) were optimized by recording the trimer's IR spectrum. UV radiation was generated by frequency doubling the output of a tunable dye laser, and frequencies were calibrated by the known REMPI spectrum of HCl. Spectra were collected by alternating "IR on" and "IR off" conditions at each frequency. In "IR on", the IR laser was fired 70 ns before the UV laser, whereas in "IR off", the IR laser was fired 2 μs after the UV laser.

Both the $f^3\Delta_2(v'=0) \leftarrow X\ ^1\Sigma^+(v''=0)$ and $V\ ^1\Sigma^+(v'=11$ and $12) \leftarrow X\ ^1\Sigma^+(v''=0)$ transitions were exploited for 2+1 REMPI detection of HCl fragments. Only transitions via the $V\ ^1\Sigma^+(v'=11$ and 12) upper state were used to determine relative populations, because the f state undergoes fast predissociation,[38,39] and no signal can be observed for $J'' > 8$. For imaging we used transitions via the $f^3\Delta_2$ state whenever possible as ionization via the $V\ ^1\Sigma^+$ state terminates in a dissociative state of the ion,[40] generating a broad background in the image. For $J'' = 10$, 11 we had to use transitions via the $V\ ^1\Sigma^+$ state for imaging, and a background subtraction method was employed as described in the Supporting Information.

The VMI arrangement consists of a four-lens ion acceleration assembly, a 60 cm field-free drift tube, and a microchannel plate (MCP) detector coupled to a CCD camera that monitors a phosphor screen.[41,42] Two-dimensional projections of the ion cloud were collected using an event counting method and reconstructed to three-dimensional images using the BASEX method.[43] Speed distributions were obtained by summing over the angular distribution for each radius, and were converted to c.m. translational energy (E_T) distributions using momentum conservation, and the appropriate Jacobian ($\propto E_T^{-1/2}$) and calibration constants.

III. THEORETICAL METHODS

The PES used to describe $(HCl)_3$ is an exact representation consisting of an experimentally accurate one-body, three semiempirical intrinsic two-body and a single high-level ab initio intrinsic three-body potential.[36] Dissociation energies were calculated using the D_e values of the PES and also complete basis set (CBS) calculations, along with numerically exact zero-point energies computed using DMC simulations[44,45] for the trimer and dimer and discrete variable calculations[46] for the monomer. Additional details of the PES and the dissociation calculations are given in Supporting Information and in ref 36.

Quasiclassical trajectories were propagated to obtain the dissociation dynamics of the HCl trimer system. Simulations were performed using the Verlet propagator with a 0.25 fs time step on the PES. The chosen time step resulted in an energy drift less than 7 cm^{-1} over the course of the simulations. Every trajectory was performed with zero-point energy (ZPE) and additional vibrational excitation energy of one local-monomer stretch; the details of this excitation will be discussed as the calculations are introduced. Note that $(HCl)_3$ is a ring with each HCl equivalent. Initial conditions for each trajectory were selected by randomly sampling normal mode coordinates and momenta, subject to the energy of a particular mode and the constraint of zero total angular momentum. Once the vibrational energy was added to the system, the normal coordinates were converted to Cartesian coordinates and the velocities adjusted to set the total angular momentum and center-of-mass (c.m.) translational energy to zero. The dissociation of the trimer was monitored with respect to the three monomer's c.m. distances. If all three distances were greater than 6.5 Å, then dissociation to three monomers occurred, but if one distance was less than 6.5 Å, then the trimer was labeled as dissociating to a dimer and monomer. This distance is sufficiently large for the intermolecular interaction to be negligible. Finally, trajectories giving any fragment (monomer or dimer) with less than ZPE were discarded.

Initial explorations of dissociation dynamics, with trajectories initiated at the global minimum, led to the finding of nanosecond lifetimes for dissociation (consistent with the experimental line width[27,28]) but much shorter lifetimes for the H−Cl stretch V−V energy transfer following the initial vibrational excitation. As noted, initially each trimer is given ZPE plus an excitation energy to a given momomer stretch. Specifically, each normal mode was given a scaled harmonic energy so that the total ZPE equals the correct one determined from the DMC simulations, and one local H−Cl stretch mode was given its ZPE plus an additional energy of 2810 cm^{-1}, corresponding to one quantum of excitation. An ensemble of 5800 trajectories were run with these initial conditions and the energies of the local H−Cl stretches were monitored as a function of time. The ensemble-averaged HCl monomer

dx.doi.org/10.1021/jp5015753 | J. Phys. Chem. A XXXX, XXX, XXX−XXX

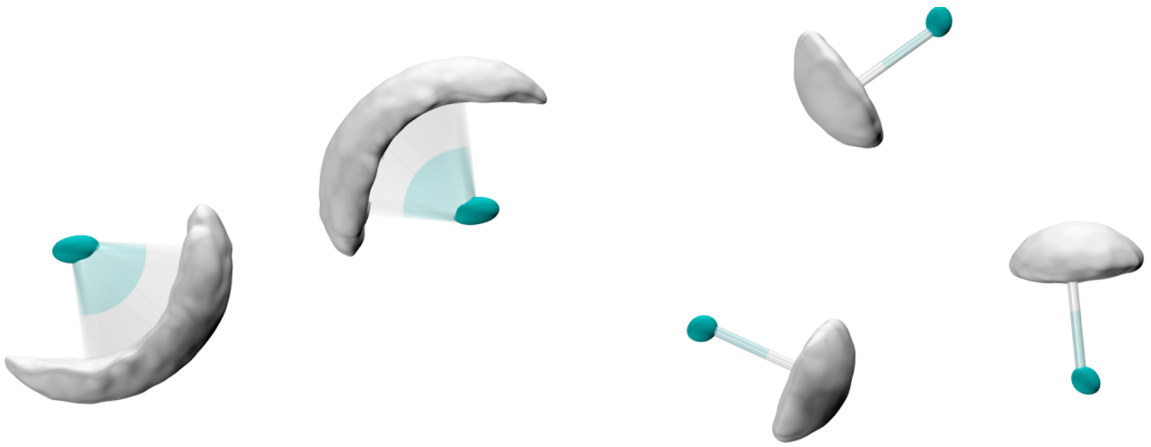

Figure 1. Isosurface representations of the HCl dimer (left) and trimer (right) ground state wave functions.

excitation energies were monitored for roughly 250 ps and ultimately fit using a single-exponential, $E = b + ae^{-k_0 t}$, and biexponential $E = b + a_1 e^{-k_1 t} + a_2 e^{-k_2 t}$ functions. The two functions were characterized by small fitting errors, less than 0.007 normalized energy units; however, the biexponential functions were able to better describe the early decay than the single exponential, as detailed below.

The next set of trajectories, using the same initial conditions as above, were performed with the goal of elucidating the VP mechanism. A set of 20 trajectories, each simulated for over 20 ns, were performed. Three of the trajectories dissociated to a monomer and a dimer, but only one with at least ZPE in the products. The remainder of the trajectories failed to dissociate. Additional shorter time scale trajectories were performed to collect dissociative "outlier" trajectories. This approach yielded an additional six trajectories that dissociated to a monomer and a dimer.

On the basis of the dissociative results, a "critical" open-chain configuration was located from which dissociation occurred. Details of this configuration are discussed below. A set of trajectories starting from this critical geometry were performed to study the energy distributions of the dissociated products. These trajectories were initiated with scaled ZPE (using the same scaling factor used at the minima) and the remaining relaxed fundamental excitation energy microcanonically distributed among the nine low-frequency modes. A total of 100 000 trajectories were performed in this manner, each propagated for 10 ps. In total 20 176 trajectories dissociated to a monomer and a dimer.

IV. RESULTS AND ANALYSIS

A. Calculations of Ground Vibrational State Wave functions. The DMC simulations allow visualization of 3D representations of the dimer and trimer vibrational ground state wave functions. Isosurfaces characterizing the two clusters are given in Figure 1. The dimer ground state wave function is highly delocalized across the two equivalent global minima resulting in two "banana" shaped proton distributions. Relative to the dimer, the trimer is much more localized with the hydrogen bonds remaining unbroken in the ground state. The protons are still delocalized about the global minimum geometry forming three "mushroom" shaped proton distributions.

B. Theoretical Description of Vibration-to-Vibration (V−V) Energy Transfer. The vibrational excitation that starts the predissociation process can be considered as being localized on a single monomer, which is coupled to the two other monomers via monomer−monomer couplings. The coupling results in V−V energy transfer between the three monomers. This ring V−V transfer has been used successfully to interpret high-resolution spectroscopic measurements of the H−Cl stretch fundamental.[27,28] It has been also observed directly in calculations using the present PES classically in the harmonic limit with just one mode excited and all other modes at equilibrium classically and also using an Huckel/exciton model very similar to the one used in the experimental analysis. The result of both simulations is a short transfer time of ∼1 ps, followed by perfect recurrences.[36] Here we examine this relaxation with the initial conditions described above. Plots of the vibrational energy relaxation and subsequent stretch relaxation are given in Figure 2. We find that the transfer

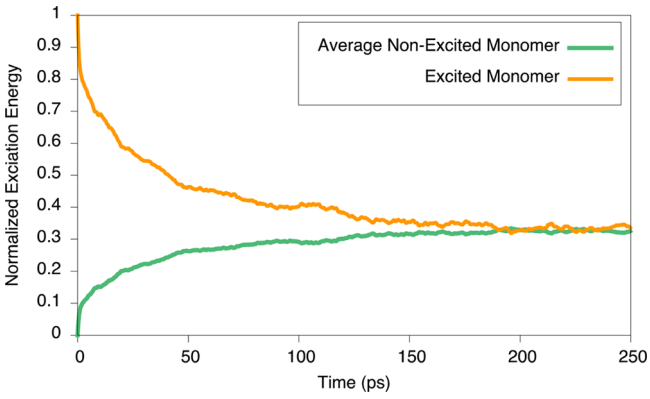

Figure 2. Vibrational energy decay and subsequent excitation of local H−Cl stretch.

process occurs first with a rapid, ∼0.7 ps, energy transfer (similar to the previously observed harmonic energy transfer process[36]) where 14% of the initial energy is removed from the initial stretch. Then a subsequent, slower energy exchange occurs, which can be described by either a single exponential with a time constant of 44 ps or a biexponential with a fast and slow component of 15 and 77 ps, respectively. Over the course of the 250 ps trajectory, the original excitation energy distributes among the H−Cl stretching modes with virtually no transfer of energy to the intermolecular modes. We do not observe the harmonic classical recurrences mentioned above,

dx.doi.org/10.1021/jp5015753 | J. Phys. Chem. A XXXX, XXX, XXX−XXX

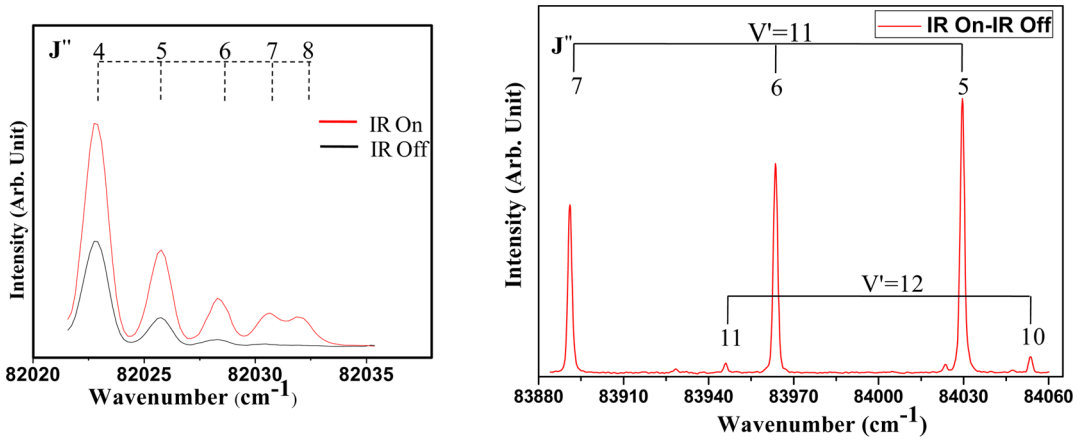

Figure 3. HCl fragment (2+1) REMPI spectrum obtained by exciting the H−Cl stretch of $(HCl)_3$ and scanning the UV laser through the $f^3\Delta_2(v'=0) \leftarrow X\ ^1\Sigma^+(v''=0)$ [left] and $V\ ^1\Sigma^+(v'=11$ and 12) $\leftarrow X\ ^1\Sigma^+(v''=0)$ [right] transitions of HCl. The left spectrum displays both "IR on" and "IR off" scans, whereas the right panel shows the "IR on"−"IR off" spectrum.

very likely because the present simulations are anharmonic and also because the ZPE motion in the intramolecular modes distorts the perfect planar ring configuration.

C. Measurements of IR Action Spectra of the Trimer. Infrared action spectra of the HCl trimer in the region of the H−Cl stretch were obtained by monitoring HCl photofragments in selected rotational states by 2+1 REMPI while scanning the IR laser frequency (action spectra), as was done previously for other clusters.[8−11,17,18,20]

Cyclic $(H^{35}Cl)_3$ has only one IR active stretch fundamental, and our observed sub-bands and band origin (2808.5 cm^{-1}) match quite well with the previously reported high-resolution gas phase spectra of 2809.8 cm^{-1},[27,28,31] and with the recently determined theoretical value (2814 cm^{-1}).[36] The IR action spectra, which are shown in Supporting Information, confirm that the enhancements observed in the signals of HCl monomers in J'' = 4−11 derive from trimer dissociation. Farnik et al.[27,28] reported a detailed rovibrational analyses and band origins for all these isotopologs, and relying on their reported band origins, we parked our IR laser at the R branch transition of $(H^{35}Cl)_3(J_{trimer}=7-10)$. In this way, we avoided exciting the other isotopolog bands except one of the split pair of the $(H^{35}Cl)_2H^{37}Cl$ (~21% of the total intensity[47]). This has been taken into account in our data analysis when necessary.

D. REMPI Spectroscopy and Rotational Distributions of HCl Fragments. As discussed earlier, two different VP channels are possible following excitation of the trimer's H−Cl stretch fundamental; Channel I (monomer + dimer) has an excess energy of ~1700 cm^{-1} [2809 to ~1100 cm^{-1}] and Channel II (three monomers) restricts the excess energy to ~1300 cm^{-1} [2809 to ~1500 cm^{-1}]. The corresponding maximum allowed J'' values for HCl from these channels are 12 and 10, respectively.

(2+1) REMPI spectra of HCl(J'') fragments obtained through the $f^3\Delta_2(v'=0) \leftarrow X\ ^1\Sigma^+(v''=0)$ and $V\ ^1\Sigma^+(v'=11$ and 12) $\leftarrow X\ ^1\Sigma^+(v''=0)$ transitions are shown in Figure 3. The spectra recorded following IR excitation show clear enhancements in J'' = 4−8 but J'' < 5 levels have large contributions from HCl monomers in the molecular beam.

The REMPI enhancement spectrum obtained via the $V\ ^1\Sigma^+$ state is shown in the right panel of Figure 3 and is assigned as transitions from J'' = 5−7 for v' = 11 ← v'' = 0 and J'' = 10 and 11 for v' = 12 ← v'' =0 transitions. Enhancement from J'' = 8, 9 (v' = 11) and J'' = 12 (v' = 12) cannot be observed due to overlap with a strong ion signal of unknown origin. The population of the highest observed rotational level, HCl-(J''=11), is small but its position matches well with published data.[48] Because the V state is less predissociative, we used the V ← X transition to estimate the relative populations of $J'' \geq 5$ levels. We did so by integrating the area under each peak, using line strength factors of 1,[48] and multiplying the populations obtained via v' = 12 excitation by a Franck−Condon factor of 1.55.[48] The relative populations of fragment HCl(J'') levels are given in Table S1 in Supporting Information. Figure 4 presents

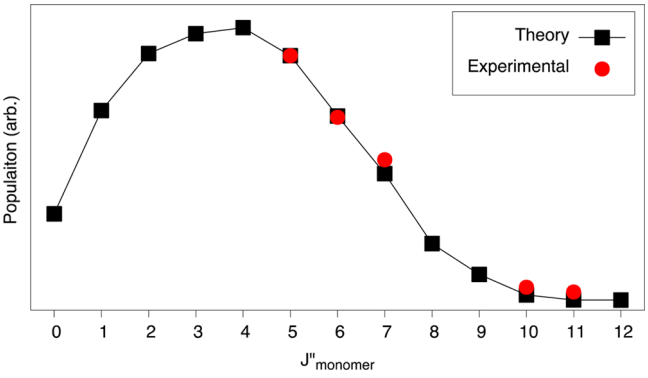

Figure 4. Comparison of theoretical and available experimental HCl monomer rotational populations.

a comparison of these populations and the relative populations computed by QCT calculations. Both theory and experiment show that the rotational populations decrease sharply for $J'' \geq$ 5, and the population of J'' = 11 is only ~5% of the population of J'' = 5. Because J'' = 11 is the only level that is associated solely with Channel I, it has special importance in image analysis, as demonstrated below. According to the calculations the HCl rotational state distribution corresponding to Channel I is broad, encompassing all the allowed states and peaking at J'' = 4.

E. Imaging Results and Dissociation Energies. Figure 5 presents velocity distributions obtained from fragment ion images recorded by monitoring several HCl(J'') levels. All the images display isotropic angular distributions, attesting to the long lifetime of the trimer.[27,28] For the reasons described above,

dx.doi.org/10.1021/jp5015753 | J. Phys. Chem. A XXXX, XXX, XXX−XXX

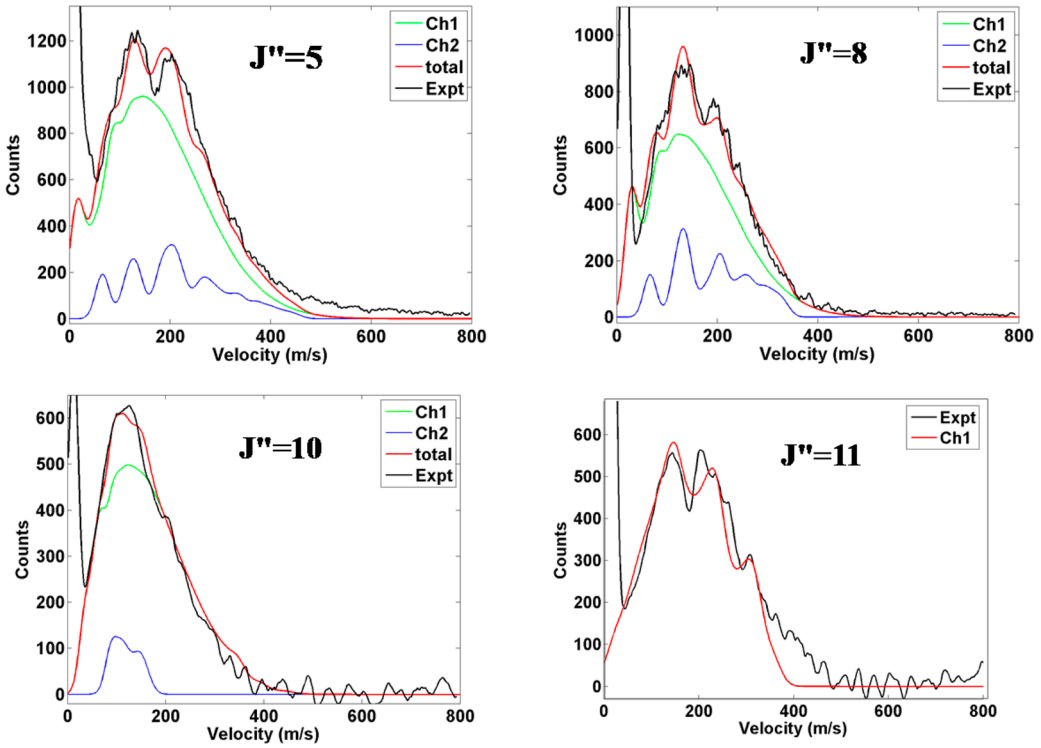

Figure 5. Velocity distributions (black curves) of state selected HCl photofragments in J'' = 5, 8, 10, and 11 rotational levels. The green and blue curves are from simulated distributions for channels I and II, respectively, and the red curve depicts the total simulated distribution, which is compared to the experimental distribution. See the text for details.

rotational levels J'' = 5 and 8 were monitored by using the $f^3\Delta_2(v'=0) \leftarrow X\ ^1\Sigma^+(v''=0)$ transition, whereas J'' = 10, 11 were detected using $V\ ^1\Sigma^+(v'=12) \leftarrow X\ ^1\Sigma^+(v''=0)$. Our previous work on dimers[8−11,17,18] shows that the dissociation energy can be determined with high accuracy when the velocity distributions display distinct and different structural features, because they all must be fit with a single value of D_0. Fortunately, this is true for most of the measured distributions, as seen in Figure 5.

The dissociation energy for Channel I, D_0(I), can be determined directly from the image of J'' = 11 for which Channel II is closed. In spite of its small population, the J'' = 11 velocity distribution shows clear and reproducible structural features that constrain the fit.

To fit the J'' = 11 image we assigned, as before, a Gaussian-shaped curve to each rotational level of each of the $(HCl)_2$ cofragment vibrational levels and determined the positions of these Gaussians using energy conservation:

$$h\nu_{IR} + E_{int}(\text{trimer}) = D_0(\text{Channel I}) + E_{rot}(\text{monomer}) + E_{vib,rot}(\text{dimer}) + E_T$$

E_{int}(trimer) is the internal energy of the trimer prior to excitation, which depends on the beam temperature and the specific excitation position of the trimer IR spectrum. $h\nu_{IR}$ is the photon energy used for the vibrational excitation of the trimer (2809 cm^{-1}), and D_0 is the dissociation energy for Channel I (monomer + dimer). E_{rot}(monomer) is the rotational energy of the monitored HCl fragment, $E_{vib,rot}$(dimer) is the rovibrational energy of the dimer cofragment, and E_T is the c.m. translational energy. State selective REMPI defines E_{rot}(monomer), and E_T is determined from the image. Therefore, D_0 and $E_{vib,rot}$(dimer) are the unknown variables in the image.

In determining $E_{vib,rot}$(dimer), we need to consider the populations of the dimer's four low-frequency intermolecular vibrations (no intramolecular vibrations are energetically allowed), and because not all have been obtained experimentally in the gas phase, we use the results of Qui et al.,[15,49] who performed six-dimensional quantum calculations and reported all the intermolecular anharmonic vibrational frequencies for the ground as well as for ν_1 and ν_2 excited $(HCl)_2$. The available experimental values[14,50−52] agree with the theoretical predictions of Qui et al.[15,49] within 2−4 cm^{-1}.[53] The dimer's rotational energy levels were calculated using the published rotational constants by Schuder et al.[54] We assigned a Gaussian shaped curve to each rotational state of $(HCl)_2$ with a width characteristic of our experimental resolution.

Figure 5 shows the best fit to the J'' = 11 distribution from which we determine D_0(I) = 1140 ± 5 cm^{-1}. The best fit to the structures in the image was obtained by using similar populations for all the fundamental intermolecular vibrations and excluding overtones and combination bands. Other dimer population distributions (e.g., including only rotational excitation, or giving equal populations to all energetically allowed vibrational levels) gave much less satisfactory fits to the data (see Supporting Information for examples). All the reasonable fits we tried changed D_0(I) only slightly, and including other sources of error described below increased the final error estimate to ±20 cm^{-1}.

All other images include contributions from both channels I and II. Because Channel I gives rise to a dimer cofragment with a high density of rovibrational states, the velocity distribution associated with it is nearly structureless. Fortunately, D_0(I) could be determined accurately from the J'' = 11 velocity

dx.doi.org/10.1021/jp5015753 | J. Phys. Chem. A XXXX, XXX, XXX−XXX

distribution, and this value was used in fitting all the other images, with the only variables in the fittings being D_0 for Channel II [D_0(II)] and the population ratio Channel I:Channel II.

The products of Channel II dissociation are three HCl monomers, resulting in unique structural features in each HCl(J'') velocity distribution. In Channel II, the cofragments are two HCl monomers and no vibrational excitation is possible. Therefore, the excess energy is distributed only among the sparse rotational levels of the two HCl cofragments (whose rotational energies are known precisely) and the c.m. E_T.

At the end of the fitting process, we further fine-tuned the dissociation energies for each individual image until we obtained the best fits. Our final dissociation energies are the average of the values obtained from several images, and image-to-image deviations are included in our error bars. All four images could be fit well with dissociation energies, 1138 and 1541 cm^{-1} for channels I and II, respectively. The estimated internal energy of the HCl trimer prior to excitation is 4 ± 3 cm^{-1} [R branch transition with J'' = 7−10] and thus our final dissociation energies are D_0(I) = 1142 ± 20 cm^{-1} and D_0(II) = 1545 ± 10 cm^{-1}. We have given a larger error bar to D_0(I) due to the uncertainty in the intermolecular vibrational frequencies of the dimer cofragments and their relative populations, and the existence of only one image with Channel I as the sole product channel.

Dissociation energies for the trimer and dimer are listed in Table 1. Two sets of theoretical dissociation energies were computed using numerically exact anharmonic ZPEs and D_e values obtained with the many-body potential (PES) and also from complete basis set calculations (CBS). The anharmonic ZPEs for the monomer, dimer and trimer are 1483, 3235 ± 1, and 5260 ± 1 cm^{-1}, respectively. Relative to harmonic ZPEs the anharmonic values are red-shifted 14 cm^{-1} in the monomer, 81 cm^{-1} in the dimer, and 106 cm^{-1} in the trimer. Both the PES and CBS dissociation energies are in excellent agreement with the experimental measurements. The more accurate CBS values deviate a maximum of 10 cm^{-1} when the theoretical and experimental error bars are considered. Additional details of the theoretical dissociation energies with respect to the error analysis and the CBS calculation are given in the Supporting Information.

Table 1. HCl Trimer and Dimer D_0 Values in Wavenumbers

system	D_0 [PES]	D_0 [CBS]	experiment
$(HCl)_3 \rightarrow 3(HCl)$	1526 ± 46	1564 ± 1	1545 ± 10
$(HCl)_3 \rightarrow HCl + (HCl)_2$	1102 ± 33	1133 ± 2	1142 ± 20
$(HCl)_2 \rightarrow 2(HCl)$	425 ± 29	431 ± 1	439 ± 1[55]

The experimental trimer dissociation energies obtained for Channels I and II and the dimer's dissociation energy of 439 cm^{-1} [55] place the cooperative (nonadditive) contribution at ~250 cm^{-1}, in good agreement with the theoretical values of ~251 and ~271 cm^{-1}, obtained for the two theoretical methods.

F. Measured and Calculated Translational Energy Distributions. Figure 6 displays the c.m. E_T distributions derived from velocity distributions of HCl fragments in different J'' levels along with the corresponding distributions obtained from the QCT calculations for Channel I. Although the experimental and theoretical distributions match quite well for J'' = 10, they deviate progressively more as the monitored J'' level decreases, with the greatest mismatch for J'' = 5.

The cause for this mismatch becomes clear when one considers the possible internal energies of the dimer cofragments associated with each monitored HCl(J'') monomer fragment. When these energies exceed the dimer's dissociation energy of ~430 cm^{-1}, the dimer will further dissociate into two monomers. The QCT calculations and the experiments show that most of the products are formed via Channel I, with a fraction of the dimer fragments having high internal energies (see also Supporting Information). When these internally "hot" dimers dissociate, they produce monomers with a broad E_T distribution extending to very low translational energies. We denote the dissociation of these "hot" dimer fragments, $[(HCl)_2]^{**}$, as Channel Ia:

$$[(HCl)_2]^{**} \rightarrow HCl + HCl \qquad \text{(Channel Ia)}$$

The final velocity of the HCl(J'') monomer generated via this pathway depends on the velocities of dimers generated in Channel I and the velocity of HCl generated via Channel Ia.

$$\vec{V}_{HCl} = \vec{V}_{HCl\,dimer} + \vec{V}_{HCl} \qquad \text{(Channel Ia)}$$

Thus, the final observed HCl(J'') velocity distributions from Channel Ia include contributions from many internal energies and velocities of the dimer, making it impossible to reconstruct the exact velocity distribution for Channel Ia. However, we can still estimate the maximum E_T via this channel from energy conservation, and predict the qualitative shape of the velocity distribution, as described below.

Referring to the HCl(J''=5) E_T distribution, and taking into account ~430 cm^{-1} for the dimer's dissociation energy and 319 cm^{-1} for the energy of the HCl(J''=5) product, we find that the contribution of Channel Ia to the J'' = 5 image can derive only from dimers with internal energies greater than ~750 cm^{-1}.

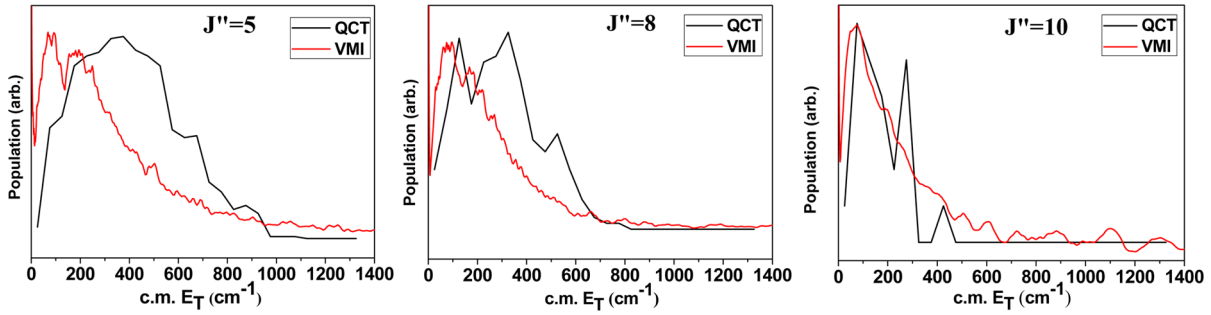

Figure 6. c.m. E_T distributions obtained by detecting HCl fragment (red curve) in J'' = 5, 8, and 10. Black curves are the corresponding distributions obtained from the QCT calculation for Channel I.

dx.doi.org/10.1021/jp5015753 | J. Phys. Chem. A XXXX, XXX, XXX−XXX

The fraction of dimers with this internal energy is small (~20%), and calculations show that it drops sharply as the internal energy increases from 800 to 1400 cm^{-1} (see Supporting Information). Thus, secondary dissociation rationalizes the low-E_T component in the observed HCl distribution. As expected, the contribution of Channel Ia decreases in going from the J'' = 5−8 images, as the latter requires a minimum dimer internal energies of ~1050 cm^{-1}, and the best agreement between theory and experiment is indeed obtained for J'' = 10.

To obtain an estimate of the velocity distribution corresponding to Channel Ia, we fitted the c.m. E_T distribution of J'' = 5 by using contributions from three channels as shown in Figure 7. For Channel I, we used the QCT calculated

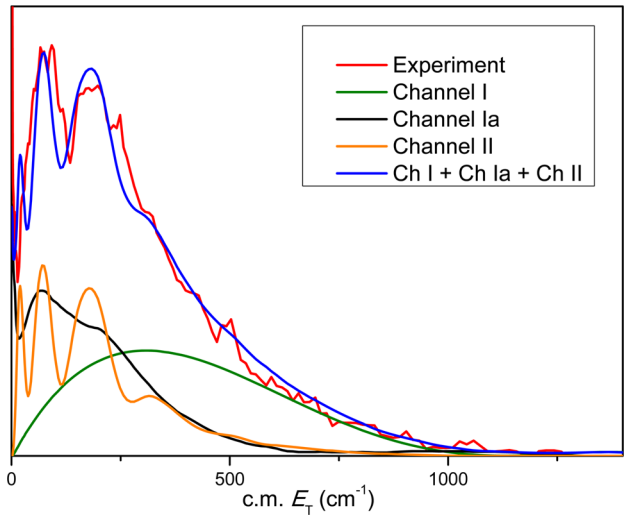

Figure 7. c.m. E_T distribution obtained by monitoring HCl in J'' = 5 (red curve), and the fitted total distribution (blue) obtained by summing contributions from Channel I (green), Ia (black), and II (orange). See the text for details.

distribution after smoothing, and scaled it to match the tail part of the distribution. The Channel II distribution was taken from the experimental fit (Figure 5) and scaled to reproduce the structure and dip in the E_T distribution. After these two partial distributions were established, the distribution corresponding to Channel Ia was generated simply by subtracting these from the measured distribution. The fitted distribution for Channel Ia shown in Figure 7 shows all the qualitative trends discussed above; i.e., it is broad and smooth with a maximum at low translational energies. This distribution also matches well with the average E_T of ~62 cm^{-1} obtained in the QCT calculation for HCl(J''=5) from Channel Ia, which is much lower than the corresponding total Channel I average E_T of ~400 cm^{-1}.

V. DISCUSSION

Previous high-resolution spectroscopic work on the ring HCl trimer focused on the initial step of V−V transfer and suggested that multiple time scales are involved in the VP.[27,28] The present work identifies the fragmentation channels of the vibrationally excited trimer and elucidates dissociation mechanisms. It demonstrates that indeed breaking up the hydrogen bonds following excitation of the H−Cl stretch of the trimer is hard and that the lifetime of the trimer is long, greater than a nanosecond. This presents a challenge for calculations as even with long simulations, i.e., greater than 20 ns, dissociation of the timer, on average, is not observed. Nevertheless, by combining theoretical and experimental results we are able to present, for the first time, a detailed picture of the dissociation process of an H-bonded network− from initial excitation to final energy distributions in the products.

The theoretical calculations show that the rate-limiting step in the VP is the transfer of H−Cl stretch excitation to the intermolecular modes of the trimer. This is in agreement with Farnik and Nesbitt,[27,28] who suggested on the basis of their spectroscopic work that V−V transfer is followed by energy transfer to low-frequency modes and then ring-opening. Indeed, simulations find that once the H−Cl stretch relaxes, one H-bond can break and the ring can transition to an open chain configuration, 737 cm^{-1} higher in energy. This conformer is stable enough to allow energy to localize and break a second H-bond, forming a monomer and dimer (Channel I). The minimum energy path to this configuration is demonstrated in Figure 8.

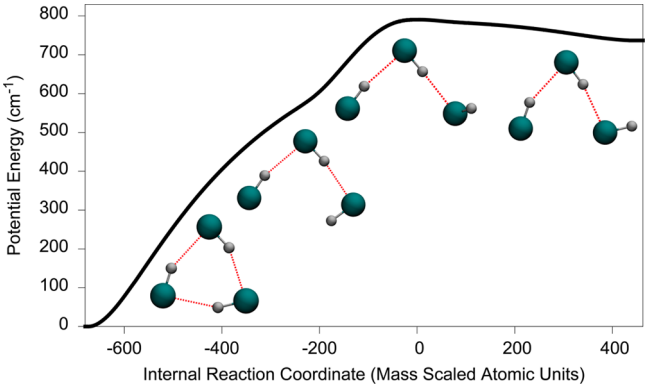

Figure 8. Minimum energy path from trimer to open-chain configuration.

Both theory and experiment indicate that the HCl dimer fragment of Channel I has a broad distribution of rovibrational energies, which indicates that the distribution resembles to a large degree a microcanonical distribution. Fits to the measured velocity distributions of specific HCl(J'') levels correlated with dimer cofragments suggest that high overtones and combination bands do not have large populations, and the major vibrational excitation involves fundamental levels of the dimer intermolecular modes.

Some dimer fragments possess internal energies greater than their dissociation energy and these dimers further dissociate to two HCl monomers. Evidence for this secondary dissociation (Channel Ia) is obtained both from experiments (Figures 6 and 7) and from the QCT calculations. The latter provide also the distribution of internal energies in the excited dimers, which in turn allows an estimation of the c.m. E_T distributions associated with Channel Ia. The calculations and experiments both indicate that this E_T distribution is structureless, extending to the maximum energy allowed by conservation of energy and peaking at low E_T (Figure 7). It should be noted that this distribution is very different from what has been observed previously in dissociation of the HCl dimer.[55] In the present calculations the dissociation starts from an excited state where energy is distributed microcanonically in all vibrations except for the H−Cl stretches, whereas in the previous experiments energy was initially deposited only in a H−Cl stretch vibration. Comparison of the two cases reveals that the form of initial

dx.doi.org/10.1021/jp5015753 | J. Phys. Chem. A XXXX, XXX, XXX−XXX

excitation greatly influences the energy disposal in the fragments.

The trajectory calculations show that even after reaching the critical configuration of the open-chain trimer, the breaking off of an HCl monomer is not instantaneous; it involves many vibrational motions, with H-bonds breaking and re-forming until finally an HCl monomer breaks off. An animation of the final picoseconds of the trimer dissociation to a monomer and a dimer is available in .avi format. Similar behavior has been found before in QCT calculations of the water trimer.[20] This may indicate a common mechanism of breakup of cyclic trimers. The measured rotational energy distribution of the HCl monomer and the c.m. E_T distributions correlated with specific HCl(J'') fragment states are quite broad, in accordance with the theoretical predictions.

The experimental results identify also a small fraction of trimers that dissociate directly to three monomers (Channel II). This channel is not seen in trajectory calculations that start from the global minimum of the trimer. This is probably because only a small number of the trajectories terminate in dissociation (<10), and this ensemble is too small to reveal minor channels. On the other hand, in the experiment Channel II is evident because it leads to distinct structures in the HCl(J'') velocity distributions. It appears that Channel II does not proceed via a sequential breaking of H-bonds (Channels I and Ia) but rather via a single step mechanism that involves the breakup of all three H bonds at the same time.

The distinct structural features that appear in the pair-correlated velocity distributions allow us to determine the dissociation energies of Channels I and II very accurately, and the experimentally determined values are in excellent agreement with theory, as are the global rotational distributions. We conclude that the new PES applied here is capable of describing accurately both spectroscopic and dynamical properties of the dissociating trimer. We are not aware of any other PES of a trimer that has been tested so rigorously by comparisons to both spectroscopic and VP observations.

Another important property of H-bonding is the nonadditive cooperative contributions. Despite ring strain, we find that the cooperative contribution is large, about 250 cm^{-1} of D_0(I) of ~1100 cm^{-1}; i.e., three-body effects contribute more than 20% to the binding strength. Again, good agreement between theory and experiment is achieved. It is noteworthy that cooperative effects of the same magnitude have been observed and calculated recently for the water trimer.[20]

In conclusion, we have demonstrated that the combination of experiment and theory can yield a wealth of information and accurate results on the detailed dissociation mechanism of the ring HCl trimer. From an experimental perspective we have shown that the VP of trimers that have distinct IR absorption features can be studied in detail by using REMPI and VMI. The theoretical calculations demonstrate that it is now possible to describe properties of clusters such as D_0 and cooperative three-body interactions with excellent accuracy. The successful description of the multichannel breakup of the benchmark HCl trimer is important also in predicting the success of calculations of dissociation dynamics of larger H-bonded networks for which experiments are becoming progressively more difficult. The excellent agreement between theory and experiment demonstrated here attests to the ability of such calculations to provide reliable values of properties and mechanisms for larger H-bonded clusters.

■ ASSOCIATED CONTENT

Ⓢ Supporting Information

IR spectra; rotational distributions; background subtraction for images and different image fitting methods; details of the potential energy surface and dissociation energy calculation. This material is available free of charge via the Internet at http://pubs.acs.org.

Ⓦ Web-Enhanced Feature

An animation of the final picoseconds of the trimer dissociation to a monomer and a dimer is available in the HTML version of the paper.

■ AUTHOR INFORMATION

Corresponding Authors

*J. M. Bowman: e-mail, joel.bowman@emory.edu.
*H. Reisler: e-mail, reisler@usc.edu.

Notes

The authors declare no competing financial interest.

■ ACKNOWLEDGMENTS

We thank Kristen Zuraski and Daniel Kwasniewski for their dedicated help in data acquisition and simulations. This material is based upon work supported by the National Science Foundation under grants No. CHE-1145227 (J.M.B.) and CHE-1265725 (H.R.).

■ REFERENCES

(1) Watson, J. D.; Crick, F. H. C. A Structure for Deoxyribose Nucleic Acid. *Nature* **1953**, *171*, 737.
(2) Ludwig, R. Water: From Clusters to the Bulk. *Angew. Chem., Int. Ed.* **2001**, *40*, 1808.
(3) Moore, T. S.; Winmill, T. F. The State of Amines in Aqueous Solution. *J. Chem. Soc., Trans.* **1912**, *101*, 1635.
(4) Pimentel, G. C. *Hydrogen Bond*; W. H. Freeman & Co Ltd, 1960.
(5) Scheiner, S. *Hydrogen Bonding: A Theoretical Perspective*; Oxford University Press, USA, 1997.
(6) Zhang, J.; Chen, P.; Yuan, B.; Ji, W.; Cheng, Z.; Qiu, X. Real-Space Identification of Intermolecular Bonding With Atomic Force Microscopy. *Science* **2013**, *342*, 611.
(7) Mancini, J. S.; Bowman, J. M. Communication: A New Ab Initio Potential Energy Surface for HCl-H_2O, Diffusion Monte Carlo Calculations of D_0 and A Delocalized Zero-Point Wavefunction. *J. Chem. Phys.* **2013**, *138*, 121102.
(8) Rocher-Casterline, B. E.; Mollner, A. K.; Ch'ng, L. C.; Reisler, H. Imaging H_2O Photofragments in the Predissociation of the HCl-H_2O Hydrogen-Bonded Dimer. *J. Phys. Chem. A* **2011**, *115*, 6903.
(9) Casterline, B. E.; Mollner, A. K.; Ch'ng, L. C.; Reisler, H. Imaging the State-Specific Vibrational Predissociation of the Hydrogen Chloride-Water Hydrogen-Bonded Dimer. *J. Phys. Chem. A* **2010**, *114*, 9774.
(10) Mollner, A. K.; Casterline, B. E.; Ch'ng, L. C.; Reisler, H. Imaging the State-Specific Vibrational Predissociation of the Ammonia-Water Hydrogen-Bonded Dimer. *J. Phys. Chem. A* **2009**, *113*, 10174.
(11) Samanta, A. K.; Ch'ng, L. C.; Reisler, H. Imaging Bond Breaking and Vibrational Energy Transfer in Small Water Containing Clusters. *Chem. Phys. Lett.* **2013**, *575*, 1.
(12) Vissers, G. W. M.; Oudejans, L.; Miller, R. E.; Groenenboom, G. C.; Van Der Avoird, A. Vibrational Predissociation in the HCl Dimer. *J. Chem. Phys.* **2004**, *120*, 9487.
(13) Reisler, H. Photofragment Spectroscopy and Predissociation Dynamics of Weakly Bound Molecules. *Annu. Rev. Phys. Chem.* **2009**, *60*, 39.

(14) Elrod, M. J.; Saykally, R. J. Vibration−Rotation−Tunneling Dynamics Calculations for the Four-Dimensional $(HCl)_2$ System: A Test of Approximate Models. *J. Chem. Phys.* **1995**, *103*, 933.
(15) Qiu, Y.; Zhang, J. Z. H.; Bačić, Z. Six-Dimensional Quantum Calculations of Vibration-Rotation-Tunneling Levels of ν_1 and ν_2 HCl-Stretching Excited $(HCl)_2$. *J. Chem. Phys.* **1998**, *108*, 4804.
(16) Pine, A. S.; Lafferty, W. J. Rotational Structure and Vibrational Predissociation in the HF Stretching Bands of the HF Dimer. *J. Chem. Phys.* **1983**, *78*, 2154.
(17) Rocher-Casterline, B. E.; Ch'ng, L. C.; Mollner, A. K.; Reisler, H. Communication: Determination of the Bond Dissociation Energy (D_0) of the Water Dimer, $(H2O)_2$, By Velocity Map Imaging. *J. Chem. Phys.* **2011**, *134*, 211101.
(18) Ch'ng, L. C.; Samanta, A. K.; Czakó, G.; Bowman, J. M.; Reisler, H. Experimental and Theoretical Investigations of Energy Transfer and Hydrogen-Bond Breaking in the Water Dimer. *J. Am. Chem. Soc.* **2012**, *134*, 15430.
(19) Michael, D. W.; Lisy, J. M. Vibrational Predissociation Spectroscopy of $(HF)_3$. *J. Chem. Phys.* **1986**, *85*, 2528.
(20) Ch'ng, L. C.; Samanta, A. K.; Wang, Y.; Bowman, J. M.; Reisler, H. Experimental and Theoretical Investigations of the Dissociation Energy (D_0) and Dynamics of the Water Trimer, $(H_2O)_3$. *J. Phys. Chem. A* **2013**, *117*, 7207.
(21) Keutsch, F. N.; Cruzan, J. D.; Saykally, R. The Water Trimer. *J. Chem. Rev.* **2003**, *103*, 2533.
(22) Case, A. S.; Heid, C. G.; Western, C. M.; Crim, F. F. Determining to Dissociation Threshold of Ammonia Trimers From Action Spectroscopy of Small Clusters. *J. Chem. Phys.* **2012**, *136*, 124310.
(23) Flynn, S. D.; Skvortsov, D.; Morrison, A. M.; Liang, T.; Choi, M. Y.; Douberly, G. E.; Vilesov, A. F. Infrared Spectra of HCl−H_2O Clusters in Helium Nanodroplets. *J. Phys. Chem. Lett.* **2010**, *1*, 2233.
(24) Quack, M.; Stohner, J.; Suhm, M. A. Analytical Three-Body Interaction Potentials and Hydrogen Bond Dynamics of Hydrogen Fluoride Aggregates, (HF)n, $n \geq 3$. *J. Mol. Struct.* **2001**, *599*, 381.
(25) Haber, T.; Schmitt, U.; Suhm, M. A. FTIR-Spectroscopy of Molecular Clusters in Pulsed Supersonic Slit-Jet Expansions. *Phys. Chem. Chem. Phys.* **1999**, *1*, 5573.
(26) Skvortsov, D.; Choi, M. Y.; Vilesov, A. F. Study of HCl Clusters in Helium Nanodroplets: Experiments and Ab Initio Calculations As Stepping Stones From Gas Phase to Bulk. *J. Phys. Chem. A* **2007**, *111*, 12711.
(27) Fárník, M.; Davis, S.; Nesbitt, D. J. High-Resolution IR Studies of Hydrogen Bonded Clusters: Large Amplitude Dynamics in $(HCl)_n$. *Faraday Discuss.* **2001**, *118*, 63.
(28) Fárník, M.; Nesbitt, D. J. Intramolecular Energy Transfer Between Oriented Chromophores: High-Resolution Infrared Spectroscopy of HCl Trimer. *J. Chem. Phys.* **2004**, *121*, 12386.
(29) Latajka, Z.; Scheiner, S. Structure, Energetics and Vibrational Spectra of H-Bonded Systems. Dimers and Trimers of HF and HCl. *Chem. Phys.* **1988**, *122*, 413.
(30) Latajka, Z.; Scheiner, S. Structure, Energetics and Vibrational Spectra of Dimers, Trimers, and Tetramers of HX (X = Cl, Br, I). *Chem. Phys.* **1997**, *216*, 37.
(31) Han, J.; Wang, Z.; Mcintosh, A. L.; Lucchese, R. R.; Bevan, J. W. Investigation of to Ground Vibrational State Structure of $H^{35}Cl$ Trimer Based On to Resolved K, J Substructure of to ν_5 Vibrational Band. *J. Chem. Phys.* **1994**, *100*, 7101.
(32) Rauk, A.; Armstrong, D. A. Electron Capture By HCl Trimers: An Ab Initio Study. *Eur. Phys. J. D* **2005**, *35*, 217.
(33) Van Der Veken, B. J.; De Munck, F. R. An Infrared Study of Monomeric and Oligomeric (n=2, 3, and 4) Hydrogen Chloride in Liquified Noble Gases. *J. Chem. Phys.* **1992**, *97*, 3060.
(34) Engdahl, A.; Nelander, B. The Far-Infrared Spectrum of the Hydrogen Chloride Trimer: A Matrix Isolation Study. *J. Phys. Chem.* **1990**, *94*, 8777.
(35) Chałasiński, G.; Cybulski, S. M.; Szczęśniak, M. M.; Scheiner, S. Nonadditive Effects in HF and HCl Trimers. *J. Chem. Phys.* **1989**, *91*, 7048.
(36) Mancini, J. S.; Bowman, J. M. A New Many-Body Potential Energy Surface for HCl Clusters and Its Application to Anharmonic Spectroscopy and Vibration−Vibration Energy Transfer in the HCl Trimer. *J. Phys. Chem. A* **2014**, DOI: 10.1021/Jp412264.
(37) Mancini, J. S.; Bowman, J. M. On-The-Fly Ab Intito Calculations of Anharmonic Vibrational Frequencies: Local-Monomer Theory and Application to HCl Clusters. *J. Chem. Phys.* **2013**, *139*, 164115.
(38) Kandel, S. A.; Rakitzis, T. P.; Lev-On, T.; Zare, R. N. Dynamics for the $Cl+C_2H_6 \rightarrow HCl + C_2H_5$ Reaction Examined Through State-Specific Angular Distributions. *J. Chem. Phys.* **1996**, *105*, 7550.
(39) Rudić, S.; Ascenzi, D.; Orr-Ewing, A. Rotational Distribution of the HCl Products From the Reaction of $Cl(^2P)$ Atoms With Methanol *J. Chem. Phys. Lett.* **2000**, *332*, 487.
(40) Romanescu, C.; Manzhos, S.; Boldovsky, D.; Clarke, J.; Loock, H.-P. Superexcited State Reconstruction of HCl Using Photoelectron and Photoion Imaging. *J. Chem. Phys.* **2004**, *120*, 767.
(41) Eppink, A. T. J. B.; Parker, D. H. Velocity Map Imaging of Ions and Electrons Using Electrostatic Lenses: Application in Photoelectron and Photofragment Ion Imaging of Molecular Oxygen. *Rev. Sci. Instrum.* **1997**, *68*, 3477.
(42) Dribinski, V.; Potter, A. B.; Fedorov, I.; Reisler, H. Two-Photon Dissociation of the NO Dimer in the Region 7.1−8.2 Ev: Excited States and Photodissociation Pathways. *J. Chem. Phys.* **2004**, *121*, 12353.
(43) Dribinski, V.; Ossadtchi, A.; Mandelshtam, V. A.; Reisler, H. Reconstruction of Abel-Transformable Images: The Gaussian Basis-Set Expansion Abel Transform Method. *Rev. Sci. Instrum.* **2002**, *73*, 2634.
(44) Kosztin, I.; Faber, B.; Schulten, K. Introduction to the Diffusion Monte Carlo Method. *Am. J. Phys.* **1996**, *64*, 633.
(45) Mccoy, A. B. Diffusion Monte Carlo Approaches for Investigating the Structure and Vibrational Spectra of Fluxional Systems. *Int. Rev. Phys. Chem.* **2006**, *25*, 77.
(46) Colbert, D. T.; Miller, W. H. A Novel Discrete Variable Representation for Quantum-Mechanical Reactive Scattering Via the S-Matrix Kohn Method. *J. Chem. Phys.* **1992**, *96*, 1982.
(47) *A complication in assigning the ir spectrum stems from the isotopic contribution of $H^{37}Cl$ and, based on natural abundances, the percent contribution of $(H^{35}Cl)_3$, $(H^{35}Cl)_2H^{37}Cl$, $H_{35}Cl(H^{37}Cl)_2$ and $(H^{37}Cl)_3$ should be 42.2%, 42.2%, 14.1% and 1.6%, respectively.*
(48) Korolik, M.; Arnold, D. W.; Johnson, M. J.; Suchan, M. M.; Reisler, H.; Wittig, C. Trapping-Desorption and Direct-Inelastic Scattering of HCl From Mgo(100). *Chem. Phys. Lett.* **1998**, *284*, 164.
(49) Qiu, Y.; Bačić, Z. Exact Six-Dimensional Quantum Calculations of the Rovibrational Levels of $(HCl)_2$. *J. Chem. Phys.* **1997**, *106*, 2158.
(50) Schuder, M. D.; Lovejoy, C. M.; Lascola, R.; Nesbitt, D. J. High Resolution, Jet-Cooled Infrared Spectroscopy of $(HCl)_2$: Analysis of ν_1 and ν_2 HCl Stretching Fundamentals, Interconversion Tunneling, and Mode-Specific Predissociation Lifetimes. *J. Chem. Phys.* **1993**, *99*, 4346.
(51) FárníK, M.; Davis, S.; Schuder, M. D.; Nesbitt, D. J. Probing Potential Surfaces for Hydrogen Bonding: Near-Infrared Combination Band Spectroscopy of Van Der Waals Stretch (ν_4) and Geared Bend (ν_5) Vibrations in $(HCl)_2$. *J. Chem. Phys.* **2002**, *116*, 6132.
(52) FárníK, M.; Davis, S.; Nesbitt, D. J. Probing Hydrogen Bond Potential Surfaces for Out-Of-Plane Geometries: Near-Infrared Combination Band Torsional (ν_6) Spectroscopy In $(HCl)_2$. *J. Chem. Phys.* **2003**, *118*, 10137.
(53) *The experimental frequencies for ν_5 and ν_6 match quite well the calculated values, as F_0 recent near-infrared spectroscopic results by nesbitt and co-workers, which provide the frequencies of ν_4, ν_5 and ν_6 vibrations for the ν_2 excited level of the HCl dimer.*
(54) Schuder, M. D.; Lovejoy, C. M.; Nelson, D. D.; Nesbitt, D. J. Symmetry Breaking in HCl and DCl Dimers: A Direct Near-Infrared Measurement of Interconversion Tunneling Rates. *J. Chem. Phys.* **1989**, *91*, 4418.
(55) Ni, H.; Serafin, J. M.; Valentini, J. J. Dynamics of the Vibrational Predissociation of HCl Dimer. *J. Chem. Phys.* **2000**, *113*, 3055.